Int. J. Solids Structures Vol. 30, No. 7, pp. 875–897, 1993
Printed in Great Britain

0020–7683/93 $6.00+ .00
Pergamon Press Ltd

THE INTERPRETATION OF OPTICAL CAUSTICS IN THE PRESENCE OF DYNAMIC NON-UNIFORM CRACK-TIP MOTION HISTORIES: A STUDY BASED ON A HIGHER ORDER TRANSIENT CRACK-TIP EXPANSION

CHENG LIU and ARES J. ROSAKIS
Graduate Aeronautical Laboratories, California Institute of Technology, Pasadena, CA 91125, U.S.A.

and

L. B. FREUND
Division of Engineering, Brown University, Providence, RI 02912, U.S.A.

(*Received* 16 *March* 1992; *in revised form* 22 *October* 1992)

Abstract—The optical method of caustics is re-examined by considering the presence of dynamic non-uniform crack-tip motion histories. Based on the higher order transient expansion obtained by Freund and Rosakis (1990, Eleventh National Congress of Applied Mechanics; 1992, *J. Mech. Phys. Solids* **40**(3), 699–719) and Rosakis *et al.* (1991, *Int. J. Fract.* **50**, R39–R45), in which dynamic transient effects were included in the near-tip deformation field, the exact mapping equations of caustics are derived for non-uniformly propagating cracks. The resulting equations indicate that the classical analysis of caustics based on the assumption of K_I^d-dominance, is inadequate to interpret the experimental caustic patterns when dynamic transient effects become significant. In this paper, an explicit relation between the instantaneous value of the dynamic stress intensity factor $K_I^d(t)$ and the geometrical characteristics of the caustic is established. This relation shows that for the case of non-uniformly propagating cracks, the relation between the dynamic stress intensity factor and the geometrical characteristics of the caustic pattern depends on the crack-tip acceleration and on $\dot{K}_I^d(t)$. It also reduces to the classical relation between $K_I^d(t)$ and the caustic diameter for the case of K_I^d-dominance (when the crack-tip fields are well described by the $r^{-1/2}$ singularity in stresses). The Broberg problem is used as an example problem to check the feasibility of analysing caustics in the presence of higher order transient terms. It is shown the value of the dynamic stress intensity factor obtained by the proposed method agrees remarkably well with the exact analytical value while large errors are introduced when the classical analysis (K_I^d-dominant) of the method of caustics is used.

1. INTRODUCTION

The optical method of caustics, a technique based on geometrical optics, has several advantages over the other light wave interference methods which are mainly related to its simplicity. It requires a simple optical set-up which does not involve the use of diffraction optics. It can be used easily either in transmission or in reflection arrangements. Data analysis is simple and does not require the use of complicated image processing techniques. The simplicity of the technique makes it an ideal candidate for high speed photography applications. In particular, the fact that the physical principle of caustics does not hinge on the availability of a coherent, monochromatic light source, has allowed for the use of high-speed camera systems which utilize white light illumination such as the Cranz–Schardin type cameras. In addition, the lack of complicated optical components, such as diffraction gratings, beam splitters, etc., in a caustic set-up ensures minimal light intensity losses which are crucial for successful high-speed photography, especially when the exposure time is in the order of nanoseconds.

The method of caustics has been initially introduced by Schardin (1959) and Manogg (1964). Manogg used caustics in a transmission arrangement and gave the first quantitative analysis. He showed that the geometrical characteristics of the caustic depend on the nature and intensity of the crack-tip singularity and was able to measure the intensity of the near-tip stress field. After Manogg's work, the method of caustics was extensively used by Theocaris, who was also the first one to use this method in a reflection arrangement (Theocaris, 1970, 1971). Later, Theocaris and Gdoutos (1974) applied the method of

caustics in reflection to experimentally examine the deformation fields near the tips of stationary cracks in metal plates, and this is the first application of the method to the investigation of fracture in metals. Since the beginning of the 1970s, the optical method of caustics has been developed into a successful experimental stress analysis method and found wide applications, especially for the analysis of dynamic fracture mechanics problems.

There are two sets of simplifying assumptions that are customarily made in the various applications of the method of caustics. One regards the analysis of the optical process (transmission or reflection) and the other regards the nature of the mechanical fields under study. In each of them, assumptions and simplifications are made in order to interpret the caustic pattern quantitatively. The limitations introduced by the simplifications in the optical analysis of the method of caustics as well as an exact geometrical optics interpretation of the technique were thoroughly discussed by Rosakis and Zehnder (1985) and Rosakis (1992). However the corresponding issue regarding the assumptions made about the mechanical fields under study is more complicated and troublesome.

In linearly elastic dynamic fracture mechanics, the method of caustics was first used in experiments involving very rapid crack propagation and stress wave loading by Kalthoff *et al.* (1976), Katsamanis *et al.* (1977), Theocaris (1978) and Goldsmith and Katsamanis (1979). In each case, it was assumed that the elastic stress field in the vicinity of a rapidly propagating crack tip has precisely the same spatial variation as the elastic stress field near the tip of a stationary crack. That is, the influence of inertial effects on the spatial distribution of the crack-tip field was not taken into account. Kalthoff *et al.* (1978) introduced an approximate correction factor to account for the error introduced when the static local field is used in the interpretation of caustic patterns. Rosakis (1980) presented the exact equations of the caustic envelope for elastic specimens containing rapidly growing cracks. He also presented the caustic equations for the case of mixed mode plane stress crack propagation. The above analyses all assume that the deformation field near the propagating crack tip is K_I^d-dominant. This means that the stress field at a finite region near the crack tip can be approximated accurately by the elastodynamic asymptotic singular solution (to within some acceptable error). Based on this assumption, many experimental investigations of the dynamic crack initiation, propagation and arrest have been carried out since then.

Recent experimental investigations by Krishnaswamy and Rosakis (1991) and analytical results by Freund and Rosakis (1990, 1992) and Rosakis *et al.* (1991) have found that the analysis of caustics based on K_I^d-dominance may not always adequately characterize the behavior of the deformation field in the vicinity of a transiently propagating dynamic crack tip. Indeed the assumption of K_I^d-dominance is often violated during dynamic crack growth. By relaxing the assumption of K_I^d-dominance, Freund and Rosakis (1992) have suggested that under fairly severe transient conditions, a representation of the crack-tip field in the form of a higher order expansion (involving time derivatives of crack-tip velocity and stress intensity factor) should be used to interpret the experimental observations.

In this paper, we re-examine the optical method of caustics by considering non-uniform crack growth histories. The formation of the caustic image is briefly reviewed. In the following sections, the exact mapping equations of caustics and the initial curve equation are derived for a non-uniformly propagating dynamic crack. This derivation is based on the theoretical results of Freund and Rosakis (1990, 1992) and Rosakis *et al.* (1991), which allow both the crack-tip speed and the dynamic stress intensity factor to be arbitrary differentiable functions of time. Then the explicit relation between the dynamic stress intensity factor, $K_I^d(t)$, and two geometrical dimensions of the caustic pattern, is established. It is shown that the classical analysis of the caustics is a special case of this result under the condition of strict K_I^d-dominance. Finally, in order to verify the accuracy of the analysis developed in this paper, the Broberg problem is considered as an example problem of transient crack growth. The exact caustic patterns are generated by using the Broberg problem. These patterns are subsequently analysed by using both the classical analysis and the improved method proposed here. The results show that the value of the dynamic stress intensity factor obtained by the proposed method agrees remarkably well with the exact analytical value while large errors are introduced when the classical analysis (K_I^d-dominance) of the method of caustics is used.

2. METHOD OF CAUSTICS

2.1. *Mapping equations*

Consider a plate specimen of uniform thickness, h, in the undeformed state. Let its mid-plane occupy the x_1, x_2-plane of an orthonormal Cartesian coordinate system. As the specimen is subjected to applied loads, non-uniform gradients in the optical path of light transmitted through it, or reflected from its surface, are generated. For a transparent specimen, the gradients in the optical path are due to non-uniform changes in the thickness of the plate and also due to stress induced gradients in the refractive index of the material in the specimen interior. For an opaque specimen, the gradients in the optical path are due to non-uniform surface elevations of the plate.

Consider further a collimated beam of light travelling in the x_3-direction, normally incident on the plate, as illustrated in Fig. 1. Under certain stress gradients, the reflected or refracted rays will deviate from parallelism and form an envelope in the form of a three-dimensional surface in space. This surface, which is called the *caustic surface*, is the locus of points of maximum luminosity in the reflected or transmitted light fields.

The deflected rays are tangential to the caustic surface. If a screen is positioned parallel to the $x_3 = 0$ plane, so that it intersects the caustic surface, then the cross-section of the surface can be observed on the screen as a bright curve (the *caustic curve*) bordering a dark region (the *shadow spot*). Suppose that the incident ray, which is reflected from or transmitted through point $p(x_1, x_2)$ on the specimen, intersects the screen at the image point $P(X_1, X_2)$. The (X_1, X_2) coordinate system is identical to the (x_1, x_2) system, except that the origin of the former has been translated by a distance z_0 from the screen (z_0 can be either positive or negative). The position of the image point P will depend on the gradient of the optical path change $\Delta S(x_1, x_2)$ introduced by the specimen as well as on the distance z_0 and is given by Rosakis and Zehnder (1985):

$$\mathbf{X} = \mathbf{x} + z_0 \nabla(\Delta S(x_1, x_2)), \tag{1}$$

where $\mathbf{X} = X_\alpha \mathbf{e}_\alpha$, $\mathbf{x} = x_\alpha \mathbf{e}_\alpha$, $\alpha = 1, 2$, and $\mathbf{e}_\alpha$ denote unit vectors, and ∇ denotes the two-dimensional gradient operator. Relation (1) describes the mapping of the points on the specimen onto the points on the screen.

2.2. *The initial curve and its significance*

If the screen intersects the caustic surface, then the resulting caustic curve on the screen is the optical mapping of the locus of points for which the determinant of the Jacobian matrix of mapping equation (1) must vanish on the specimen, i.e.

$$J(x_1, x_2; z_0) = \det[x_{\alpha,\beta}] = \det[\delta_{\alpha\beta} + z_0(\Delta S)_{,\alpha\beta}] = 0. \tag{2}$$

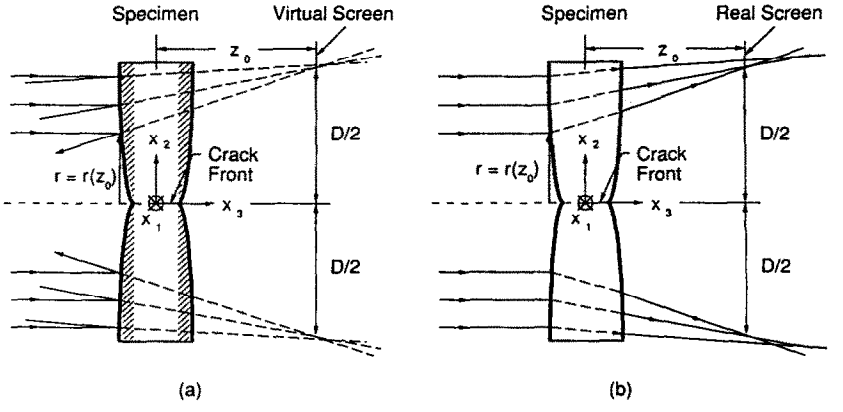

(a) (b)

Fig. 1. Caustic formation in (a) reflection, (b) transmission.

Equation (2) is a necessary and sufficient condition for the existence of a caustic curve. The locus of points on the reference plane $(x_1, x_2, x_3 = 0)$ for which the Jacobian vanishes is called the *initial curve* whose geometry is described by eqn (2). All points on the initial curve map onto the caustic curve. In addition, all points inside and outside this curve map *outside* the caustic (Rosakis and Zehnder, 1985). Since the light transmitted through or reflected from both the interior and the exterior of the initial curve maps only outside the caustic, the area within the caustic remains dark and is customarily referred to as the shadow spot. Also, since the light that forms the caustic curve originates from the initial curve, essential information conveyed by the caustic comes from that curve only.

Equation (2), defining the initial curve, depends parametrically on z_0. Thus, by varying z_0, we may vary the initial curve position. If z_0 is large, the initial curve will be far from the crack tip. If z_0 is small, the initial curve will be close to the crack tip. Variation of z_0 can easily be achieved experimentally by simply varying the focal plane of the recording camera system. This is an essential property of the method of caustics, and it can be utilized to "scan" the near-tip region to obtain information regarding the nature of the deformation field at different distances from the crack tip. For the present work, we require that the initial curve is located outside the near-tip plastic and three-dimensional zones.

3. INTERPRETATION OF CAUSTIC PATTERNS IN THE PRESENCE OF TRANSIENT EFFECTS

3.1. *Caustics generated by non-uniformly propagating cracks*

For opaque specimens, caustics are formed by the reflection of light rays from the polished specimen surface. The shape of the caustic curve depends on the near-tip normal displacement u_3 of the plate surface, initially at $x_3 = h/2$, where h is the undeformed specimen thickness. For transparent specimens the optical path change ΔS depends on both local changes in thickness and on local changes in the refractive index. The change in the refractive index Δn is given by the Maxwell relation:

$$\Delta n(x_1, x_2) = D_1(\sigma_{11} + \sigma_{22} + \sigma_{33}),$$

where D_1 is the stress optic constant and σ_{ij} are the nominal stress components. The above relation is strictly true for mechanically and optically isotropic linear elastic solids.

For a cracked linear elastic plate of uniform thickness and finite in-plane dimensions, the optical path difference ΔS, in general, will depend on the details of the three-dimensional elastostatic or elastodynamic stress state that would exist at the vicinity of the crack tip. This will be a function of the applied loading, in-plane dimensions and thickness of the specimen. In the present work, we assume that the two-dimensional asymptotic analyses provide adequate approximations for $\Delta S(x_1, x_2)$. In particular, it has been suggested that the conditions of generalized plane stress will dominate in thin cracked plates at distances from the crack tip larger than half of the specimen thickness (Rosakis and Ravi-Chandar, 1986; Yang and Freund, 1985), which implies that if the initial curve is kept outside the near-tip three-dimensional zone, the resulting caustic could be interpreted as the basis of a generalized plane stress analysis. Furthermore, in this paper, we also assume that the initial curve is always kept outside the plastic and the fracture process zones, and this enables the asymptotic elastic analysis to be employed to interpret the caustic pattern.

Under the aforementioned conditions, the optical path difference $\Delta S(x_1, x_2)$ will be (Rosakis, 1992):

$$\Delta S(x_1, x_2) = ch[\hat{\sigma}_{11}(x_1, x_2) + \hat{\sigma}_{22}(x_1, x_2)], \tag{3}$$

where

$$c = \begin{cases} \left(D_1 - \dfrac{\nu}{E}(n-1)\right) = c_\sigma & \text{for transmission,} \\ \dfrac{\nu}{E} & \text{for reflection,} \end{cases}$$

and E and ν are the Young's modulus and the Poisson's ratio of the material respectively,

c_σ is called the stress-optical coefficient, and $\hat{\sigma}_{11}$ and $\hat{\sigma}_{22}$ are thickness averages of the stress components in the solid. These stress components will be provided by the generalized plane stress solution of the elastostatic or elastodynamic problem under investigation.

Consider a planar, mode-I crack that grows through a two-dimensional, homogeneous, isotropic, linearly elastic solid, with a non-uniform speed $v(t)$, along the positive x_1-direction. (x_1, x_2) is a coordinate system which translates with the moving crack tip. The asymptotic stress around the tip of a non-uniformly propagating dynamic crack was presented by Rosakis *et al.* (1991). Let the scaled polar coordinate system (r_l, θ_l) and (r_s, θ_s) be defined as:

$$r_{l,s}^2(t) = x_1^2 + \alpha_{l,s}^2(t)x_2^2,$$

$$\theta_{l,s}(t) = \tan^{-1}\left\{\frac{\alpha_{l,s}(t)x_2}{x_1}\right\},$$

$$\alpha_{l,s}^2(t) = 1 - \frac{v^2(t)}{c_{l,s}^2},$$

where c_l and c_s are the longitudinal and shear stress wave velocities of the elastic material, respectively. Then, the first stress invariant corresponding to the fully transient dynamic crack is (Freund and Rosakis, 1992):

$$\frac{\hat{\sigma}_{11}+\hat{\sigma}_{22}}{2\rho(c_l^2-c_s^2)} = \frac{3v^2}{4c_l^2}A_0(t)r_l^{-1/2}\cos\frac{\theta_l}{2} + \frac{2v^2}{c_l^2}A_1(t)$$
$$+\left\{\frac{15v^2}{4c_l^2}A_2(t)\cos\frac{\theta_l}{2} + D_l^1\{A_0(t)\}\left[\left(1-\frac{v^2}{2c_l^2}\right)\cos\frac{\theta_l}{2} + \frac{v^2}{8c_l^2}\cos\frac{3\theta_l}{2}\right]\right.$$
$$\left.+\frac{1}{2}B_l(t)\left[\left(1-\frac{v^2}{c_l^2}\right)\cos\frac{\theta_l}{2} - \left(1-\frac{5v^2}{8c_l^2}\right)\cos\frac{3\theta_l}{2} + \frac{v^2}{16c_l^2}\cos\frac{7\theta_l}{2}\right]\right\}r_l^{1/2} + O(r_l), \quad (4)$$

where

$$A_0(t) = \frac{4}{3\mu\sqrt{2\pi}}\frac{1+\alpha_s^2}{D(v)}K_I^d(t),$$

$$D_l^1\{A_0(t)\} = -\frac{3v^{1/2}(t)}{\alpha_l^2 c_l^2}\frac{d}{dt}\{v^{1/2}(t)A_0(t)\}$$
$$= -\frac{4v^{1/2}(t)}{\mu\sqrt{2\pi}\alpha_l^2 c_l^2}\frac{d}{dt}\left\{v^{1/2}(t)\frac{1+\alpha_s^2}{D(v)}K_I^d(t)\right\},$$

$$B_l(t) = \frac{3v^2(t)}{2\alpha_l^4 c_l^4}A_0(t)\frac{dv(t)}{dt} = \frac{2v^2(t)}{\mu\sqrt{2\pi}\alpha_l^4 c_l^4}\frac{1+\alpha_s^2}{D(v)}K_I^d(t)\frac{dv(t)}{dt},$$

$$D(v) = 4\alpha_l\alpha_s - (1+\alpha_s^2)^2,$$

and $K_I^d(t)$ is the dynamic stress intensity factor at the crack tip, ρ and μ are the mass density and the shear modulus of the elastic material, respectively.

By substituting the above expression for the first stress invariant into the optical path difference relation (3), the mapping equation (1) becomes:

$$X_l = r_l\cos\theta_l + z_0 ch\rho(c_l^2-c_s^2)\left[\frac{3v^2}{4c_l^2}A_0(t)r_l^{-3/2}\cos\frac{3\theta_l}{2}\right.$$
$$\left.-\left\{D_l^1\{A_0(t)\}\left[\left(1-\frac{v^2}{4c_l^2}\right)\cos\frac{\theta_l}{2} - \frac{v^2}{8c_l^2}\cos\frac{5\theta_l}{2}\right]\right.\right.$$

$$-\frac{1}{2}B_1(t)\left[\left(1-\frac{v^2}{4c_1^2}\right)\cos\frac{\theta_1}{2}-\left(1-\frac{3v^2}{8c_1^2}\right)\cos\frac{5\theta_1}{2}+\frac{3v^2}{16c_1^2}\cos\frac{9\theta_1}{2}\right]$$

$$+\frac{15v^2}{4c_1^2}A_2(t)\cos\frac{\theta_1}{2}\Big\}r_1^{-1/2}\Big], \tag{5}$$

$$X_2=\frac{r_1\sin\theta_1}{\alpha_1}+\alpha_1 z_0 ch\rho(c_1^2-c_s^2)\left[\frac{3v^2}{4c_1^2}A_0(t)r_1^{-3/2}\sin\frac{3\theta_1}{2}\right.$$

$$-\left\{D_1^1\{A_0(t)\}\left[\left(1-\frac{3v^2}{4c_1^2}\right)\sin\frac{\theta_1}{2}-\frac{v^2}{8c_1^2}\sin\frac{5\theta_1}{2}\right]\right.$$

$$+\frac{1}{2}B_1(t)\left[3\left(1-\frac{3v^2}{4c_1^2}\right)\sin\frac{\theta_1}{2}+\left(1-\frac{7v^2}{8c_1^2}\right)\sin\frac{5\theta_1}{2}-\frac{3v^2}{16c_1^2}\sin\frac{9\theta_1}{2}\right]$$

$$+\frac{15v^2}{4c_1^2}A_2(t)\sin\frac{\theta_1}{2}\Big\}r_1^{-1/2}\Big]. \tag{6}$$

The initial curve defined by eqn (2) is:

$$1+z_0 ch\rho(c_1^2-c_s^2)\left\{-\frac{9v^4}{8c_1^4}A_0(t)r_1^{-5/2}\cos\frac{5\theta_1}{2}+\left[\frac{15v^4}{8c_1^4}A_2(t)\cos\frac{3\theta_1}{2}\right.\right.$$

$$\left.-D_1^1\{A_0(t)\}(f^{\mathrm{d}}_{11}(\theta_1)+\alpha_1^2 f^{\mathrm{d}}_{22}(\theta_1))+B_1(t)(f^{\mathrm{b}}_{11}(\theta_1)-\alpha_1^2 f^{\mathrm{b}}_{22}(\theta_1))\right]r_1^{-3/2}\Big\}$$

$$+\alpha_1^2[z_0 ch\rho(c_1^2-c_s^2)]^2\left\{-\left(\frac{9v^2}{8c_1^2}A_0(t)\right)^2 r_1^{-5}+\frac{9v^2}{8c_1^2}A_0(t)\left[\frac{15v^2}{4c_1^2}A_2(t)\cos\theta_1\right.\right.$$

$$\left.-D_1^1\{A_0(t)\}g_1^{\mathrm{d}}(\theta_1)+B_1(t)g_1^{\mathrm{b}}(\theta_1)\right]r_1^{-4}+\left[-\left(\frac{15v^2}{8c_1^2}A_2(t)\right)^2+\frac{15v^2}{8c_1^2}A_2(t)D_1^1\{A_0(t)\}g_2^{\mathrm{d}}(\theta_1)\right.$$

$$+(D_1^1\{A_0(t)\})^2[f^{\mathrm{d}}_{11}(\theta_1)f^{\mathrm{d}}_{22}(\theta_1)-(f^{\mathrm{d}}_{12}(\theta_2))^2]$$

$$-B_1(t)\left\{\frac{15v^2}{8c_1^2}A_2(t)g_2^{\mathrm{b}}(\theta_1)+D_1^1\{A_0(t)\}[f^{\mathrm{d}}_{22}(\theta_1)f^{\mathrm{b}}_{11}(\theta_1)-f^{\mathrm{d}}_{11}(\theta_1)f^{\mathrm{b}}_{22}(\theta_1)\right.$$

$$\left.\left.\left.-2f^{\mathrm{d}}_{12}(\theta_1)f^{\mathrm{b}}_{12}(\theta_1)]\right\}-B_1^2(t)[f^{\mathrm{b}}_{11}(\theta_1)f^{\mathrm{b}}_{22}(\theta_1)+(f^{\mathrm{b}}_{12}(\theta_1))^2]\right]r_1^{-3}\right\}=0, \tag{7}$$

where

$$g_1^{\mathrm{d}}(\theta_1)=(f^{\mathrm{d}}_{11}(\theta_1)-f^{\mathrm{d}}_{22}(\theta_1))\cos\frac{5\theta_1}{2}+2f^{\mathrm{d}}_{12}(\theta_1)\sin\frac{5\theta_1}{2},$$

$$g_1^{\mathrm{b}}(\theta_1)=(f^{\mathrm{b}}_{11}(\theta_1)+f^{\mathrm{b}}_{22}(\theta_1))\cos\frac{5\theta_1}{2}+2f^{\mathrm{b}}_{12}(\theta_1)\sin\frac{5\theta_1}{2},$$

$$g_2^{\mathrm{d}}(\theta_1)=(f^{\mathrm{d}}_{11}(\theta_1)-f^{\mathrm{d}}_{22}(\theta_1))\cos\frac{3\theta_1}{2}+2f^{\mathrm{d}}_{12}(\theta_1)\sin\frac{3\theta_1}{2},$$

$$g_2^{\mathrm{b}}(\theta_1)=(f^{\mathrm{b}}_{11}(\theta_1)+f^{\mathrm{b}}_{22}(\theta_1))\cos\frac{3\theta_1}{2}+2f^{\mathrm{b}}_{12}(\theta_1)\sin\frac{3\theta_1}{2},$$

$$f^{\mathrm{d}}_{11}(\theta_1)=-\frac{1}{2}\cos\frac{3\theta_1}{2}+\frac{3v^2}{16c_1^2}\cos\frac{7\theta_1}{2},$$

$$f^{b}_{11}(\theta_1) = -\frac{3}{4}\left(1-\frac{v^2}{3c_1^2}\right)\cos\frac{3\theta_1}{2} + \frac{3}{4}\left(1-\frac{v^2}{8c_1^2}\right)\cos\frac{7\theta_1}{2} - \frac{15v^2}{64c_1^2}\cos\frac{11\theta_1}{2},$$

$$f^{d}_{22}(\theta_1) = \frac{1}{2}\left(1-\frac{v^2}{c_1^2}\right)\cos\frac{3\theta_1}{2} - \frac{3v^2}{16c_1^2}\cos\frac{7\theta_1}{2},$$

$$f^{b}_{22}(\theta_1) = \frac{5}{4}\left(1-\frac{4v^2}{5c_1^2}\right)\cos\frac{3\theta_1}{2} + \frac{3}{4}\left(1-\frac{9v^2}{8c_1^2}\right)\cos\frac{7\theta_1}{2} - \frac{15v^2}{64c_1^2}\cos\frac{11\theta_1}{2},$$

$$f^{d}_{12}(\theta_1) = -\frac{1}{2}\left(1-\frac{v^2}{2c_1^2}\right)\sin\frac{3\theta_1}{2} + \frac{3v^2}{16c_1^2}\sin\frac{7\theta_1}{2},$$

$$f^{b}_{12}(\theta_1) = \frac{1}{4}\left(1-\frac{v^2}{2c_1^2}\right)\sin\frac{3\theta_1}{2} + \frac{3}{4}\left(1-\frac{5v^2}{8c_1^2}\right)\sin\frac{7\theta_1}{2} - \frac{15v^2}{64c_1^2}\sin\frac{11\theta_1}{2}.$$

In the expressions above, $A_0(t)$ is determined by the dynamic stress intensity factor history, $K_I^d(t)$, and the propagating speed of the crack tip, $v(t)$. $D_1^1\{A_0(t)\}$ depends not only on $K_I^d(t)$ and $v(t)$, but also on the time derivatives of these quantities. Besides $K_I^d(t)$ and $v(t)$, $B_1(t)$ also depends on the acceleration of the crack. From the first stress invariant, eqn (4), we can see that the dynamic transient effects, $D_1^1\{A_0(t)\}$ and $B_1(t)$ inter the expression only through the second and the third terms. If we also want to investigate the higher order time derivatives of $K_I^d(t)$ and $v(t)$, we have to use higher order terms in the asymptotic expansion of stress. The coefficients $A_1(t)$ and $A_2(t)$ are undetermined by the asymptotic analysis. Their values can only be determined for particular initial/boundary value problems. It should be observed at this point that the θ_1 variation of the higher order terms in relation (4) is different from that of the steady-state higher order expansion presented by Dally *et al.* (1985). Relation (4) reduces to the steady-state case only if both K_I^d and v are constant.

From the expressions above, we can also see that if the crack-tip speed $v(t)$ is a constant, i.e. $\dot{v}(t) = 0$, and therefore $B_1(t) = 0$, eqns (5), (6) and (7) give the caustic mapping equation and the initial curve equation corresponding to transient crack growth under constant velocity and varying stress intensity factor. Furthermore, if the time derivative of the dynamic stress intensity factor, $\dot{K}_I^d(t)$ is also zero, $D_1^1\{A_0(t)\}$ will be zero. In such a case, eqns (5), (6) and (7) describe the caustic curves corresponding to steady-state crack growth evaluated on the basis of a three term steady-state expansion for the stresses. If in addition, A_2 vanishes, these relations exactly reduce to the results obtained under the assumption of K_I^d-dominance (Rosakis, 1980). For stationary cracks ($v = 0$), $D_1^1\{A_0(t)\}$ and $B_1(t)$ all vanish even if $\dot{K}_I \neq 0$. Depending on whether the loading is dynamic or not, A_2 may be either a constant or a function of time. If A_2 happens to vanish, then a situation of K_I-dominance is established outside the near tip three-dimensional zone and the equations of the caustics reduce to those of an epicycloid (Theocaris, 1981).

3.2. *Relation between the dynamic stress intensity factor and the geometrical dimensions of caustics*

For a given specimen with a straight mode-I crack, if the initial conditions and the boundary conditions are prescribed, and also if the crack propagation history, i.e. the propagating velocity of the crack tip $v(t)$, is known, then the history of the dynamic stress intensity factor, $K_I^d(t)$, can be determined. Consequently, $D_1^1\{A_0(t)\}$ and $B_1(t)$, which depend on the dynamic stress intensity factor and the crack-tip velocity as well as on their time derivatives, can also be determined, and so can the coefficients $A_1(t)$ and $A_2(t)$. According to eqns (5), (6) and (7), the shape of the initial curve and the caustic pattern corresponding to this dynamic crack propagation process for each instant of time can be calculated. However, in laboratory situations the inverse problem is encountered. That is, the values of $K_I^d(t)$, $D_1^1\{A_0(t)\}$, $B_1(t)$, $A_1(t)$ and $A_2(t)$ have to be determined from the caustic pattern. Indeed, in dynamic fracture experiments we need to establish a method of

infering the stress intensity factor history from local near tip measurements, since the boundary/initial value problem is usually too difficult to solve. In this section, we provide the main steps of the derivation of the relation between the dynamic stress intensity factor and some experimentally measurable quantities (i.e. geometrical characteristics of caustic and crack-tip velocity).

Since the caustic mapping equations (5) and (6), and the initial curve equation (7) are too complicated, we now make the assumption that $v/c_1 \ll 1$. This assumption is realistic since in most solids terminal crack growth velocities do not exceed a speed of $0.2c_1$, or approximately $0.5c_R$ before branching. c_R is the material Rayleigh wave speed in plane stress. It is thus felt that assuming that $v/c_1 \ll 1$ will lead to a useful and accurate simplification for the mapping equations. By making this simplification, eqns (5) and (6) become:

$$X_1 = r_1\cos\theta_1 + \hat{K}(t)r_1^{-3/2}\cos\frac{3\theta_1}{2} - \hat{A}(t)r_1^{-1/2}\cos\frac{\theta_1}{2} - \frac{1}{2}\hat{B}(t)r_1^{-1/2}\left(\cos\frac{\theta_1}{2} - \cos\frac{5\theta_1}{2}\right), \quad (8)$$

$$X_2 = \frac{r_1\sin\theta_1}{\alpha_1} + \alpha_1\left\{\hat{K}(t)r_1^{-3/2}\sin\frac{3\theta_1}{2} - \hat{A}(t)r_1^{-1/2}\sin\frac{\theta_1}{2} + \frac{1}{2}\hat{B}(t)r_1^{-1/2}\left(3\sin\frac{\theta_1}{2} + \sin\frac{5\theta_1}{2}\right)\right\}, \quad (9)$$

and the initial curve equation associated with the above mapping equations are obtained by requiring that the Jacobian of the above transformation vanishes, i.e.

$$\begin{aligned}
&\left\{1 - \frac{3}{2}(1-\alpha_1^2)\hat{K}(t)r_1^{-5/2}\cos\frac{5\theta_1}{2} - \frac{9}{4}\alpha_1^2\hat{K}^2(t)r_1^{-5}\right\} \\
&+ \left\{\frac{1}{2}(1-\alpha_1^2)\hat{A}(t)r_1^{-3/2}\cos\frac{3\theta_1}{2} + \frac{3}{2}\alpha_1^2\hat{K}(t)\hat{A}(t)r_1^{-4}\cos\theta_1 - \frac{1}{4}\alpha_1^2\hat{A}^2(t)r_1^{-3}\right\} \\
&- \hat{B}(t)\left\{\frac{1}{4}\left[(3+5\alpha_1^2)\cos\frac{3\theta_1}{2} - 3(1-\alpha_1^2)\cos\frac{7\theta_1}{2}\right]r_1^{-3/2} - 3\alpha_1^2\hat{K}(t)r_1^{-4}\cos\theta_1\right. \\
&\left. + \frac{1}{4}\hat{A}(t)(1+3\cos 2\theta_1)r_1^{-3} + \frac{1}{8}\hat{B}(t)(1+3\cos 2\theta_1 - 4\cos 3\theta_1)r_1^{-3}\right\} = 0, \quad (10)
\end{aligned}$$

where

$$\begin{aligned}
\hat{K}(t) &= z_0 ch\rho(c_1^2 - c_s^2)\frac{3v^2}{4c_1^2}A_0(t) = \frac{z_0 chF(v)}{\sqrt{2\pi}}K_1^d(t), \\
\hat{A}(t) &= z_0 ch\rho(c_1^2 - c_s^2)\left\{\frac{15v^2}{4c_1^2}A_2(t) + D_1^1\{A_0(t)\}\right\}, \\
\hat{B}(t) &= z_0 ch\rho(c_1^2 - c_s^2)B_1(t), \\
F(v) &= \frac{(\alpha_1^2 - \alpha_s^2)(1+\alpha_s^2)}{4\alpha_1\alpha_s - (1+\alpha_s^2)^2}.
\end{aligned}$$

Now, given experimentally obtained caustic patterns and an appropriate numerical scheme, eqns (8), (9) and (10) can be used to obtain the values of $\hat{K}(t)$, $\hat{A}(t)$ and $\hat{B}(t)$ as functions of time.

Since the initial curve equation (10) is still too complicated to use, and in an attempt to retain some of the simplicity of the classical analysis of caustics one can introduce a simplifying assumption regarding the nature of the initial curve by assuming that the initial curve remains a circle of radius $r_0(t)$, i.e.

$$r_1 = (\tfrac{3}{2}\alpha_1 \hat{K}(t))^{2/5} = r_0(t), \tag{11}$$

which implies that the size of the initial curve is only determined by the instantaneous value of the dynamic stress intensity factor, as well as the propagating velocity of the crack tip, rather than the time derivatives of these quantities. By substituting $r_1 = r_0(t)$ into the mapping equations (8) and (9), the parametric equations of the caustic are obtained as follows:

$$X_1 = r_0\left\{\cos\theta_1 + \frac{2}{3\alpha_1}\left[\cos\frac{3\theta_1}{2} - \frac{\hat{A}(t)r_0}{\hat{K}(t)}r_0\cos\frac{\theta_1}{2} - \frac{\hat{B}(t)}{2\hat{K}(t)}\left(\cos\frac{\theta_1}{2} - \cos\frac{5\theta_1}{2}\right)\right]\right\}, \tag{12}$$

$$X_2 = r_0\left\{\frac{\sin\theta_1}{\alpha_1} + \frac{2}{3}\left[\sin\frac{3\theta_1}{2} - \frac{\hat{A}(t)r_0}{\hat{K}(t)}\sin\frac{\theta_1}{2} + \frac{\hat{B}(t)r_0}{2\hat{K}(t)}\left(3\sin\frac{\theta_1}{2} + \sin\frac{5\theta_1}{2}\right)\right]\right\}. \tag{13}$$

For $\hat{A}(t)r_0/\hat{K}(t) \to 0$ and $\hat{B}(t)r_0/\hat{K}(t) \to 0$, eqns (12) and (13) reduce to the parametric equations for dynamic caustics obtained on the basis of K_1^d-dominance (Rosakis, 1980). The validity of the assumption regarding the circularity of the initial curve will be justified in Section 4 in connection with the Broberg problem.

The two caustic curve dimensions chosen in this analysis are the maximum transverse diameter D of the caustic and the distance between the point of intersection of this diameter with the X_1-axis and the front point of the caustic. This length will be denoted by X. These lengths are shown in Fig. 2. If the end point of the caustic diameter has coordinates $X_1^{(D)}$ and $X_2^{(D)}$, respectively, and if the front point of the caustic curve, has coordinates $X_1^{(F)}$ and $X_2^{(F)} = 0$, then one can use the mapping equations (8) and (9) to write:

$$X_1^{(F)} = r_0 + \hat{K}(t)r_0^{-3/2} - \hat{A}(t)r_0^{-1/2}, \tag{14}$$

$$X_2^{(F)} = 0, \tag{15}$$

$$X_1^{(D)} = r_0\cos\theta_1^{(D)} + \hat{K}(t)r_0^{-3/2}\cos\frac{3\theta_1^{(D)}}{2} - \hat{A}(t)r_0^{-1/2}\cos\frac{\theta_1^{(D)}}{2} - \frac{1}{2}\hat{B}(t)r_0^{-1/2}\left(\cos\frac{\theta_1^{(D)}}{2} - \cos\frac{5\theta_1^{(D)}}{2}\right), \tag{16}$$

$$X_2^{(D)} = \frac{r_0\sin\theta_1^{(D)}}{\alpha_1} + \alpha_1\left\{\hat{K}(t)r_0^{-3/2}\sin\frac{3\theta_1^{(D)}}{2} - \hat{A}(t)r_0^{-1/2}\sin\frac{\theta_1^{(D)}}{2} + \frac{1}{2}\hat{B}(t)r_0^{-1/2}\left(3\sin\frac{\theta_1^{(D)}}{2} + \sin\frac{5\theta_1^{(D)}}{2}\right)\right\}, \tag{17}$$

where $\theta_1^{(D)}$ is the angular coordinate of the point $(r_0, \theta_1^{(D)})$ on the initial curve that maps

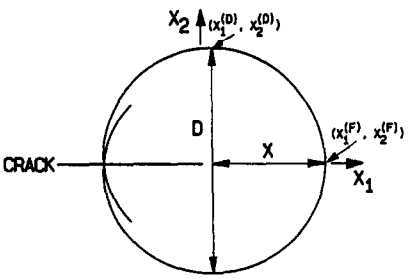

Fig. 2. Evaluation of the dynamic stress intensity factor $K_1^d(t)$ by measuring two geometrical dimensions, D and X.

onto the point $(X_1^{(D)}, X_2^{(D)})$, where X_2 is maximum. Since at this point, X_2 is a local maximum, the following condition has to be met:

$$\frac{\partial X_2}{\partial \theta_1} = 0, \quad \text{for } \theta_1 = \theta_1^{(D)}. \tag{18}$$

The relations between the experimentally measurable quantities, D and X, and the points $(X_1^{(D)}, X_2^{(D)})$ and $(X_1^{(F)}, X_2^{(D)})$, are:

$$D = 2X_2^{(D)}, \tag{19}$$

$$X = X_1^{(F)} - X_1^{(D)}. \tag{20}$$

Then, the relations that should be used to obtain the unknown coefficients are:

$$\frac{D}{r_0} = 2\left(\frac{\sin\theta_1^{(D)}}{\alpha_1} + \frac{2}{3}\sin\frac{3\theta_1^{(D)}}{2}\right) - 2\alpha_1\hat{A}(t)r_0^{-3/2}\sin\frac{\theta_1^{(D)}}{2} + \alpha_1\hat{B}(t)r_0^{-3/2}\left(3\sin\frac{\theta_1^{(D)}}{2} + \sin\frac{5\theta_1^{(D)}}{2}\right), \tag{21}$$

$$\frac{X}{r_0} = \left(1 + \frac{2}{3\alpha_1} - \cos\theta_1^{(D)} - \frac{2}{3\alpha_1}\cos\frac{3\theta_1^{(D)}}{2}\right) - \hat{A}(t)r_0^{-3/2}\left(1 - \cos\frac{\theta_1^{(D)}}{2}\right) + \frac{1}{2}\hat{B}(t)r_0^{-3/2}\left(\cos\frac{\theta_1^{(D)}}{2} - \cos\frac{5\theta_1^{(D)}}{2}\right) \tag{22}$$

and

$$\frac{1}{r_0}\left(\frac{\partial X_2}{\partial \theta_1}\right)_{\theta_1=\theta_1^{(D)}} = \left(\frac{\cos\theta_1^{(D)}}{\alpha_1} + \cos\frac{3\theta_1^{(D)}}{2}\right) - \frac{1}{2}\alpha_1\hat{A}(t)r_0^{-3/2}\cos\frac{\theta_1^{(D)}}{2} + \frac{1}{4}\alpha_1\hat{B}(t)r_0^{-3/2}\left(3\cos\frac{\theta_1^{(D)}}{2} + 5\cos\frac{5\theta_1^{(D)}}{2}\right) = 0. \tag{23}$$

In the above expressions, relation (11) between $\hat{K}(t)$ and r_0 has been used. It seems that there are only three equations, (21), (22) and (23), but four undetermined parameters, r_0 (or $\hat{K}(t)$), $\theta_1^{(D)}$, $\hat{A}(t)$ and $\hat{B}(t)$. However, if the crack propagating velocity, $v(t)$ and thus $\dot{v}(t)$ are independently known, then $\hat{B}(t)$ is related to $\hat{K}(t)$ by:

$$\hat{B}(t) = \frac{2\dot{v}(t)}{\alpha_1^4 c_1^2}\hat{K}(t),$$

and thus $\hat{B}(t)$ and $\hat{K}(t)$ are not independent variables. So actually there are only three undetermined parameters, and they can be obtained by solving eqns (21), (22) and (23). By eliminating $\hat{A}(t)$ and $\hat{B}(t)$ from eqns (21), (22) and (23), we obtain the relations:

$$\frac{D}{r_0} = \left\{g_1(\theta_1^{(D)}) - 2g_1'(\theta_1^{(D)})\tan\frac{\theta_1^{(D)}}{2}\right\} + \frac{2\dot{v}(t)D}{\alpha_1^4 c_1^2}\left\{g_2(\theta_1^{(D)}) - 2g_2'(\theta_1^{(D)})\tan\frac{\theta_1^{(D)}}{2}\right\}\frac{r_0}{D}, \tag{24}$$

$$\frac{X}{r_0} = f_1(\theta_1^{(D)}) + \frac{2\dot{v}(t)X}{\alpha_1^4 c_1^2} f_2(\theta_1^{(D)})\frac{r_0}{X}, \tag{25}$$

where

$$g_1(\theta_1^{(D)}) = 2\left(\frac{\sin\theta_1^{(D)}}{\alpha_1} + \frac{2}{3}\sin\frac{3\theta_1^{(D)}}{2}\right),$$

$$g_2(\theta_1^{(D)}) = \frac{2}{3}\left(3\sin\frac{\theta_1^{(D)}}{2} + \sin\frac{5\theta_1^{(D)}}{2}\right),$$

$$f_1(\theta_1^{(D)}) = 1 + \frac{2}{3\alpha_1} - \left[1 + \frac{2}{\alpha_1^2}\left(\sec\frac{\theta_1^{(D)}}{2} - 1\right)\right]\cos\theta_1^{(D)} + \frac{2}{\alpha_1}\left(\frac{2}{3} - \sec\frac{\theta_1^{(D)}}{2}\right)\cos\frac{3\theta_1^{(D)}}{2},$$

$$f_2(\theta_1^{(D)}) = \frac{1}{3\alpha_1}\left\{\left(4 - 3\sec\frac{\theta_1^{(D)}}{2}\right)\cos\frac{\theta_1^{(D)}}{2} + \left(4 - 5\sec\frac{\theta_1^{(D)}}{2}\right)\cos\frac{5\theta_1^{(D)}}{2}\right\}.$$

In the above expressions, the prime denotes differentiation with respect to the argument $\theta_1^{(D)}$. Consequently, when D and X are measured, r_0 and $\theta_1^{(D)}$ can be obtained by solving eqns (24) and (25), and therefore, the dynamic stress intensity factor, $K_1^d(t)$, can be obtained from relation (11).

To be more explicit, we solve eqn (24) for r_0, which then can be expressed as:

$$r_0 = \frac{D}{g_1(\theta_1^{(D)})}\left\{1 - \frac{2g_1'(\theta_1^{(D)})}{g_1(\theta_1^{(D)})}\tan\frac{\theta_1^{(D)}}{2}\right\}^{-1}\left\{\frac{1}{2} + \sqrt{\frac{1}{4} + \frac{2\dot{v}(t)D}{\alpha_1^4 c_1^2}\frac{G_2(\theta_1^{(D)})}{[G_1(\theta_1^{(D)})]^2}}\right\}^{-1}, \tag{26}$$

where

$$G_1(\theta_1^{(D)}) = g_1(\theta_1^{(D)}) - 2g_1'(\theta_1^{(D)})\tan\frac{\theta_1^{(D)}}{2},$$

$$G_2(\theta_1^{(D)}) = g_2(\theta_1^{(D)}) - 2g_2'(\theta_1^{(D)})\tan\frac{\theta_1^{(D)}}{2}.$$

By using eqns (11) and (26), the dynamic stress intensity factor can be expressed as:

$$K_1^d(t) = \frac{2\sqrt{2\pi}}{3\alpha_1 chz_0 F(v)}\left\{\frac{D}{g_1(\theta_1^{(D)})}\right\}^{5/2}\left\{1 - \frac{2g_1'(\theta_1^{(D)})}{g_1(\theta_1^{(D)})}\tan\frac{\theta_1^{(D)}}{2}\right\}^{-5/2}$$
$$\times\left\{\frac{1}{2} + \sqrt{\frac{1}{4} + \frac{2\dot{v}(t)D}{\alpha_1^4 c_1^2}\frac{G_2(\theta_1^{(D)})}{[G_1(\theta_1^{(D)})]^2}}\right\}^{-5/2}. \tag{27}$$

The above expression still contains an undetermined parameter, $\theta_1^{(D)}$. However, if eqn (25) is solved for r_0, we have:

$$r_0 = \frac{X}{f_1(\theta_1^{(D)})}\left\{\frac{1}{2} + \sqrt{\frac{1}{4} + \frac{2\dot{v}(t)X}{\alpha_1^4 c_1^2}\frac{f_2(\theta_1^{(D)})}{[f_1(\theta_1^{(D)})]^2}}\right\}^{-1}.$$

Consequently, the angle $\theta_1^{(D)}$ that appears in the above equations is the root of the following trigonometric equation:

$$\frac{X}{D} = \frac{f_1(\theta_1^{(D)})}{G_1(\theta_1^{(D)})}\left\{\frac{1}{2} + \sqrt{\frac{1}{4} + \frac{2\dot{v}(t)X}{\alpha_1^4 c_1^2}\frac{f_2(\theta_1^{(D)})}{[f_1(\theta_1^{(D)})]^2}}\right\}\times\left\{\frac{1}{2} + \sqrt{\frac{1}{4} + \frac{2\dot{v}(t)D}{\alpha_1^4 c_1^2}\frac{G_2(\theta_1^{(D)})}{[G_1(\theta_1^{(D)})]^2}}\right\}^{-1}. \tag{28}$$

Under the fully transient dynamic condition, eqns (27) and (28) give the final relation between the dynamic stress intensity factor, $K_1^d(t)$, and the experimentally measurable quantities, D and X.

It should be pointed out that for the case of a non-uniformly propagating crack, the dynamic stress intensity factor, $K_1^d(t)$ measured from the caustic patterns, is explicitly

related to the crack-tip acceleration, $\dot{v}(t)$. It is also implicitly related (through $\theta_1^{(D)}$) to $\dot{K}_I^d(t)$. The coefficient $A_2(t)$ can also be obtained in the following way:

$$\hat{A}(t) = \frac{1}{\alpha_1}\sec\frac{\theta_1^{(D)}}{2}\left\{g_1'(\theta_1^{(D)})\left(\frac{r_0}{D}\right)^{3/2} + \frac{2\dot{v}(t)D}{\alpha_1^4 c_1^2} g_2'(\theta_1^{(D)})\left(\frac{r_0}{D}\right)^{5/2}\right\} D^{3/2} \tag{29}$$

and

$$A_2(t) = \frac{4c_1^2}{15v^2}\left\{\frac{\hat{A}(t)}{z_0 ch\rho(c_1^2 - c_s^2)} + \frac{8v^{1/2}(t)}{3\alpha_1^2}\frac{d}{dt}\left[\frac{v^{-3/2}(t)}{\alpha_1}\left(\frac{r_0}{D}\right)^{5/2} D^{5/2}\right]\right\}, \tag{30}$$

where r_0/D is given by eqn (26) and $\theta_1^{(D)}$ by eqn (28) in terms of the measurable quantities X and D. Once the caustic diameter D is measured at different times, $A_2(t)$ is determined from (30), provided that many sequential measurements of caustic patterns are available and if the time derivative in the formula can be evaluated by some numerical procedures.

In an experimental situation, caustic patterns are photographed and D and X are measured. Equation (28) is then used to obtain $\theta_1^{(D)}$, substitute it into eqn (27) and thus obtain $K_I^d(t)$. From eqns (29) and (30), coefficient $A_2(t)$ can also be determined.

For the case of constant velocity, $\hat{B}(t) = 0$ ($\dot{v}(t) = 0$), eqn (27) corresponds to transient crack growth under constant velocity and varying stress intensity factor. Equation (30) then gives an explicit relation between X/D and $\theta_1^{(D)}$. If the time derivative of the stress intensity factor, $\dot{K}_I^d(t)$, is also zero (steady state), then $D_1^1\{A_0(t)\} = 0$. For both $\dot{v}(t) = 0$ and steady state, the relation between the dynamic stress intensity factor, $K_I^d(t)$, and the caustic diameter, D, have the same form. The only difference comes in the value of $\theta_1^{(D)}$, which is directly related to the ratio X/D. For the transient constant velocity case ($\dot{v}(t) = 0$, $\dot{K}_I^d(t) \neq 0$):

$$A_2(t) = \frac{4c_1^2}{15v^2}\left\{\frac{\hat{A}(t)}{z_0 ch\rho(c_1^2 - c_s^2)} + \frac{8}{3\alpha_1^3 v}\frac{d}{dt}\left[\left(\frac{D}{G_1(\theta_1^{(D)})}\right)^{5/2}\right]\right\}. \tag{31}$$

For the steady state case ($\dot{v}(t) = 0$, $\dot{K}_I^d(t) = 0$):

$$A_2 = \frac{4c_1^2}{15v^2}\frac{\hat{A}}{z_0 ch\rho(c_1^2 - c_s^2)}, \tag{32}$$

or, in this case, A_2 is directly related to the caustic diameter.

Furthermore, if we only retain the singular term in the asymptotic stress expansion, then in the caustic mapping equations (8) and (9), and the initial curve equation (10) $\hat{A}(t)$ and $\hat{B}(t)$ will be zero, and eqns (8), (9) and (10) reduce to the same equations used in the classical analysis (Rosakis, 1980). If we still make the assumption of (11), the unknown parameters will reduce to two (i.e. $K_I^d(t)$ and $\theta_1^{(D)}$), and so we only need to measure one quantity from the caustic pattern, say the diameter, D. By using eqns (21) and (23), the dynamic stress intensity factor corresponding to the classical analysis can be determined. Now eqn (27) becomes:

$$K_I^d(t) = \frac{2\sqrt{2\pi}}{3\alpha_1 ch z_0 F(v)}\left\{\frac{D}{g_1(\theta_1^{(D)})}\right\}^{5/2}. \tag{33}$$

Also, if $\hat{A}(t)$ and $\hat{B}(t)$ are set to zero, the maximum condition (23) requires that

$$g_1'(\theta_1^{(D)}) = 2\left(\frac{\cos\theta_1^{(D)}}{\alpha_1} + \cos\frac{3\theta_1^{(D)}}{2}\right) = 0 \tag{34}$$

and this will provide the value of $\theta_1^{(D)}$ as a function of crack-tip velocity, v. Now define

$$C(v) = \frac{1}{\alpha_1 F(v)} \left\{ \frac{3.17}{g_1(\theta_1^{(D)})} \right\}^{5/2},$$

where $C(v)$ is a function of the crack-tip velocity, v. Equation (33) can be rewritten as:

$$K_I^d(t) = C(v) \frac{D^{5/2}}{10.7 z_0 ch}, \tag{35}$$

which has the same form as that given by Rosakis *et al.* (1984). Equation (35) is the result of the classical analysis of the caustic pattern and is widely used in the experimental interpretation of caustics corresponding to elastodynamic crack propagation.

Moreover, as $v = 0$ (stationary crack), $\alpha_1 = 1$, $F(v) = 1$ and $g_1'(\theta_1^{(D)}) = 0$, which gives $\theta_1^{(D)} = \theta_0 = 72°$, and $g_1(\theta_1^{(D)}) = 3.17$, then $C(0) = 1$ and (Theocaris, 1981; Beinert and Kalthoff, 1981):

$$K_I^d(t) = \frac{2\sqrt{2\pi}}{3chz_0} \left(\frac{D}{3.17} \right)^{5/2}. \tag{36}$$

This equation holds not only for the stationary crack subjected to dynamic loading, but also for the static problem, where $K_I^d(t)$ should be replaced by K_I.

4. AN EXAMPLE: THE BROBERG PROBLEM

4.1. *The caustic pattern corresponding to the Broberg problem*

In order to illustrate the effect of the higher order terms in caustic patterns obtained for the case of highly transient crack growth problems, and to check the ability of eqns (27) and (28) to furnish the correct values of $K_I^d(t)$, the solution of a particular elastodynamic boundary value problem is considered. This is the plane stress problem of a crack growing symmetrically from zero initial length at constant velocity under uniform remote tensile stress σ_∞. The plane of deformation is the x_1', x_2'-plane and the crack lies in the interval $-vt < x_1' < vt$, $x_2' = 0$, where v is the constant speed of either crack tip. This is the problem first analysed by Broberg (1960).

An expression for the first stress invariant directly ahead of the crack tips is obtained by Freund (1990). On the line $x_2' = 0$:

$$\sigma_{11} + \sigma_{22} = -2\sigma_\infty \frac{I(v/c_s)}{v} \left(1 - \frac{c_s^2}{c_1^2} \right) \int_{1/c_1}^{t/x_1'} \frac{f(\xi)}{(v^{-1} - \xi)^{3/2}} \, d\xi, \tag{37}$$

where $I(v/c_s)$ is a known function of v, and

$$f(\xi) = \frac{(c_s^{-2} - 2\xi^2)}{(\xi^2 - c_1^{-2})^{1/2} (v^{-1} + \xi)^{3/2}}.$$

Focusing on the crack tip moving in the positive x_1'-direction, and expanding eqn (37) in powers of $x_1 = x_1' - vt$ near $x_1 = 0$, we obtain:

$$\sigma_{11} + \sigma_{22} = W(v) \frac{K_I^d(t)}{\sqrt{2\pi}} \left\{ x_1^{-1/2} + \frac{1}{vt} \left[\frac{1}{2} + \frac{f'(1/v)}{v f(1/v)} \right] x_1^{1/2} \right\} + o(x_1^{1/2}), \tag{38}$$

where

$$W(v) = \frac{2(1 + \alpha_s^2)(\alpha_1^2 - \alpha_s^2)}{D(v)}, \tag{39}$$

$$K_I^d(t) = \frac{c_s^2 I(v/c_s) D(v)}{\alpha_1 v^2} \sigma_\infty \sqrt{\pi v t}. \tag{40}$$

If the expansion (38) is compared with the general expansion (4), in which $B_1(t) = 0$ ($\dot{v}(t) = 0$), and $\theta_1 = 0$, $r_1 = x_1$, and terms of like powers in distance from the crack tip are collected, then explicit relations for the coefficients in the expansion are obtained as:

$$A_0(t) = \frac{2}{3}\frac{W(v)}{\alpha_1^2 - \alpha_s^2}\frac{K_I^d(t)}{\mu\sqrt{2\pi}} = \frac{2\sqrt{2}}{3}\frac{(1+\alpha_s^2) I(v/c_s)}{\alpha_1(1-\alpha_s^2)}\frac{\sigma_\infty}{\mu}\sqrt{vt},$$

$$D_1^1\{A_0(t)\} = \left(1 - \frac{1}{\alpha_1^2}\right)\frac{W(v)}{\alpha_1^2 - \alpha_s^2}\frac{K_I^d(t)}{\mu\sqrt{2\pi v t}} = -\sqrt{2}\frac{(1-\alpha_1^2)(1+\alpha_s^2) I(v/c_s)}{\alpha_1^3(1-\alpha_s^2)}\frac{\sigma_\infty}{\mu}\frac{1}{\sqrt{vt}},$$

$$A_1(t) = 0,$$

$$A_2(t) = \frac{2}{15}\left[\frac{5}{4} + \frac{5}{4\alpha_1^2} + \frac{f'(1/v)}{v f(1/v)}\right]\frac{W(v)}{\alpha_1^2 - \alpha_s^2}\frac{K_I^d(t)}{\mu\sqrt{2\pi v t}}$$

$$= \frac{2\sqrt{2}}{15}\left[\frac{5}{4} + \frac{5}{\alpha_1^2} + \frac{f'(1/v)}{v f(1/v)}\right]\frac{(1+\alpha_s^2) I(v/c_s)}{\alpha_1(1-\alpha_s^2)}\frac{\sigma_\infty}{\mu}\frac{1}{\sqrt{vt}}.$$

Since the coefficients of $D_1^1\{A_0(t)\}$ and $A_2(t)$ are proportional to $1/\sqrt{t}$, the third term in the near tip asymptotic expansion of the first stress invariant is very large during the early stages of crack growth, possibly dominating the square root singular term. As a result, even though the crack-tip speed is constant, transient effects do exist in the near tip field.

For this particular problem, we normalize the caustic mapping equations (5) and (6), and the initial curve equation (7) with the length $r_0 = (3\alpha_1 \hat{K}/2)^{2/5}$. This length is related to the value of the dynamic stress intensity factor, $K_I^d(t)$, of the Broberg problem by eqn (11).

The normalized caustic mapping equations and the initial curve equation then become:

$$\frac{X_1}{r_0} = \left(\frac{r_1}{r_0}\right)\cos\theta_1 + \frac{2}{3\alpha_1}\left(\frac{r_1}{r_0}\right)^{-3/2}\cos\frac{3\theta_1}{2} - \frac{2}{3\alpha_1}\left(\frac{r_0}{vt_1}\right)\left\{\left[\frac{5}{4} + \frac{5}{4\alpha_1^2} + \frac{f'(1/v)}{v f(1/v)}\right]\cos\frac{\theta_1}{2}\right.$$

$$\left. - 2\left[\left(1 - \frac{v^2}{4c_1^2}\right)\cos\frac{\theta_1}{2} - \frac{v^2}{8c_1^2}\cos\frac{5\theta_1}{2}\right]\right\}\left(\frac{r_1}{r_0}\right)^{-1/2}, \tag{41}$$

$$\frac{X_2}{r_0} = \left(\frac{r_1}{r_0}\right)\frac{\sin\theta_1}{\alpha_1} + \frac{2}{3}\left(\frac{r_1}{r_0}\right)^{-3/2}\sin\frac{3\theta_1}{2} - \frac{2}{3}\left(\frac{r_0}{vt}\right)\left\{\left[\frac{5}{4} + \frac{5}{4\alpha_1} + \frac{f'(1/v)}{v f(1/v)}\right]\sin\frac{\theta_1}{2}\right.$$

$$\left. - 2\left[\left(1 - \frac{3v^2}{4c_1^2}\right)\sin\frac{\theta_1}{2} - \frac{v^2}{8c_1^2}\sin\frac{5\theta_1}{2}\right]\right\}\left(\frac{r_1}{r_0}\right)^{-1/2}, \tag{42}$$

and

$$\left\{1 - \frac{1}{\alpha_1}\left(\frac{v^2}{c_1^2}\right)\left(\frac{r_1}{r_0}\right)^{-5/2}\cos\frac{5\theta_1}{2} - \left(\frac{r_1}{r_0}\right)^{-5}\right\} + \frac{1}{3\alpha_1}\left(\frac{r_0}{vt}\right)\left\{\left[\left(\frac{v^2}{c_1^2}\right)\left(\frac{5}{4} + \frac{5}{4\alpha_1^2} + \frac{f'(1/v)}{v f(1/v)}\right)\cos\frac{3\theta_1}{2}\right.\right.$$

$$\left. + \frac{4}{\alpha_1}(f_{11}^d(\theta_1) + \alpha_1^2 f_{22}^d(\theta_1))\right]\left(\frac{r_1}{r_0}\right)^{-3/2} + 2\left[\left(\frac{5}{4} + \frac{5}{4\alpha_1^2} + \frac{f'(1/v)}{v f(1/v)}\right)\cos\theta_1 + \frac{2}{\alpha_1^2}g_1^d(\theta_1)\right]\left(\frac{r_1}{r_0}\right)^{-4}\right\}$$

$$- \frac{1}{9}\left(\frac{r_0}{vt}\right)^2\left\{\left(\frac{5}{4} + \frac{5}{4\alpha_1^2} + \frac{f'(1/v)}{v f(1/v)}\right)^2 + \frac{4}{\alpha_1^2}\left(\frac{5}{4} + \frac{5}{4\alpha_1^2} + \frac{f'(1/v)}{v f(1/v)}\right)g_2^d(\theta_1)\right.$$

$$\left. - \frac{16}{\alpha_1^4}[f_{11}^d(\theta_1) f_{22}^d(\theta_1) - (f_{12}^d(\theta_1))^2]\right\}\left(\frac{r_1}{r_0}\right)^{-3} = 0, \tag{43}$$

where the functions $f^{d}_{\alpha\beta}(\theta_1)$, and $g^{d}_{\alpha}(\theta_1)$ are defined in the previous section [see eqn (7)]. We can see that the coefficients of higher order terms in the non-dimensional caustic mapping equations and the initial curve equation, are proportional to a non-dimensional parameter r_0/vt. Relations (40) and (11) provide an expression for r_0/vt with respect to time after crack initiation and z_0 as follows:

$$\frac{r_0}{vt} = \left\{\frac{3}{4\sqrt{2}} \frac{(1+\alpha_s^2)I(v/c_s)}{1-\alpha_s^2} \frac{c\sigma_\infty}{1-\nu}\right\}^{2/5} \left(\frac{\sqrt{z_0 h}}{c_s t}\right)^{4/5}, \tag{44}$$

where c is a material constant and is given by eqn (3). For a given experimental set up and specimen, c, σ_∞ and h are fixed. In particular the distance between the specimen and the focal plane of the recording camera, z_0, is set prior to the experiment.

As $t \to \infty$, the ratio r_0/vt vanishes and eqns (41)–(43) reduce to the classical analysis of dynamic caustics obtained on the basis of K^{d}_{I}-dominance. Indeed this is consistent with the fact that as $t \to \infty$,

$$\dot{K}^{d}_{I}(t) = \frac{\sqrt{\pi}}{2} \frac{I(v/c_s)D(v)\sigma_\infty}{\alpha_1(1-\alpha_s^2)} \sqrt{\frac{v}{t}} \to 0,$$

which indicates that steady-state and K^{d}_{I}-dominant conditions are approached. For a fixed time $t > 0$, the ratio r_0/vt may vanish only as $z_0 \to 0$. For this case, the initial curve shrinks to the crack tip and even if $\dot{K}^{d}_{I}(t) \neq 0$, the caustic is generated from a K^{d}_{I}-dominant region. For a fixed z_0, at short times after crack initiation, $r_0/vt \to \infty$ ($\dot{K}^{d}_{I}(t) \to \infty$), and therefore transient effects are predominant. So the change of the non-dimensional parameter r_0/vt from zero to infinity characterizes the relative influence of transients on caustic shape and size.

A qualitative discussion of the influence of higher order terms and crack-tip velocity on the caustic and initial curve shapes is presented in Figs 3 and 4. Figure 3 shows the influence of crack-tip velocity on the caustic mapping for $r_0/vt = 0.3$. It is obvious that in the range $0.1 \leqslant v/c_s \leqslant 0.5$, changes in crack-tip velocity do not markedly influence the caustic shape. The initial curve also remains almost circular. The results displayed in Fig. 4 are more striking. Here, the crack-tip velocity is fixed ($v/c_s = 0.3$). The ratio r_0/vt is varied to investigate the effect of transients. Indeed, variation of r_0/vt from 0 to 1.0 creates rather

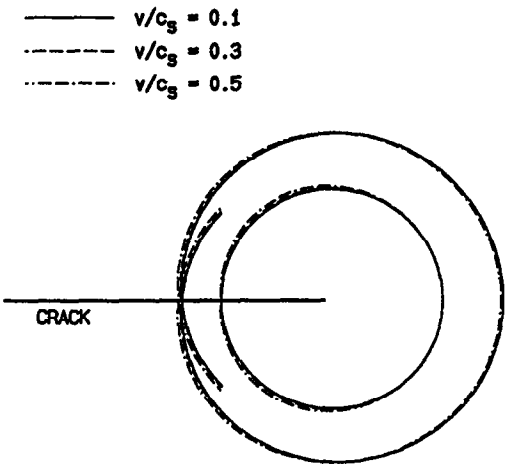

Fig. 3. Three-term simulations of the initial and caustic curves corresponding to the Broberg problem for different crack-tip velocities, and for $r_0/vt = 0.3$.

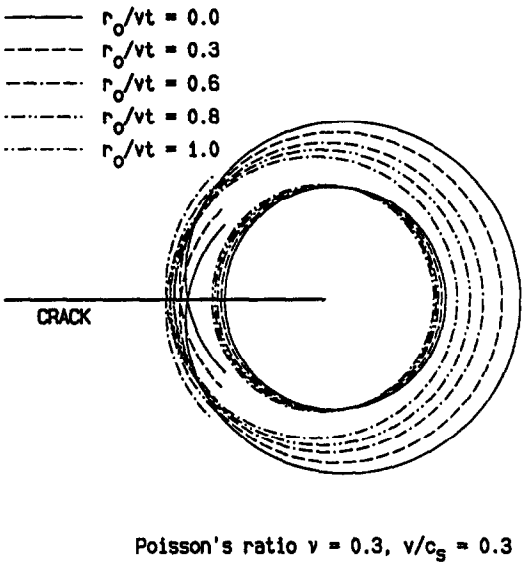

Fig. 4. Three-term simulations of the initial and caustic curves corresponding to the Broberg problem for different values of r_0/vt, which represents the scale of the transient effects, and for $v/c_s = 0.3$.

large variations in caustic shape. The value of $r_0/vt = 0$ corresponds to the caustic shape obtained by the classical (K_I^d-dominant) analysis of caustics. The differences in D and X observed for other values of r_0/vt are an indication of the error in K_I^d measurement if the classical analysis of caustics is used. On the other hand, it is very interesting to note that the initial curve is hardly influenced by the value of r_0/vt. It remains almost perfectly circular with a radius $r_1 = r_0$ as assumed by eqn (11) of our analysis. The center of the circle is moved backwards slightly as the value r_0/vt becomes relatively larger. The major assumption pivotal to the derivation of the relation between $K_I^d(t)$, D and X [eqns (27) and (28)] is the circularity of the initial curve [eqn (11)], and we feel that this provides a strong justification for our simplifying assumption.

4.2. *Comparison of the dynamic stress intensity factor obtained from different measurement methods*

The main purpose of this section is to verify the feasibility and accuracy of the measurement method proposed in Section 3.2 [eqns (27) and (28)]. This method provides a relation between the dynamic stress intensity factor at the tip of a transiently propagating crack in terms of experimentally measurable dimensions of the caustic curve. We are also interested in comparing values of K_I^d obtained from various measurement techniques, and to access their relative accuracy. More specifically, the classical analysis of caustics, which is based on the assumption of K_I^d-dominance, will be compared with the method presented above. To implement this objective, the exact caustic patterns are generated for the Broberg problem by using eqns (41), (42) and (43). Then measurements are performed on these exact caustic patterns either by the classical analysis method or by the method proposed here.

In the classical analysis of the caustic pattern, the only quantity to be measured is the diameter of the caustics, D, and this quantity is related to the dynamic stress intensity factor, $K_I^d(t)$ by relation (35) for different crack propagating velocities. In the method presented in Section 3.2 [eqns (27) and (28)], the determination of $K_I^d(t)$ also requires the evaluation of another parameter, $\theta_1^{(D)}$. To calculate $\theta_1^{(D)}$, two dimensions of the caustic need to be measured. One is the transverse diameter, D, and the other, X, is the distance from the intersection of this diameter with the X_1-axis to the front point of the caustics. The parameter $\theta_1^{(D)}$ is then given by solving eqn (28), which involves D and X as well as their ratio. Since the velocity of the crack is constant in the Broberg problem, eqn (28) implies

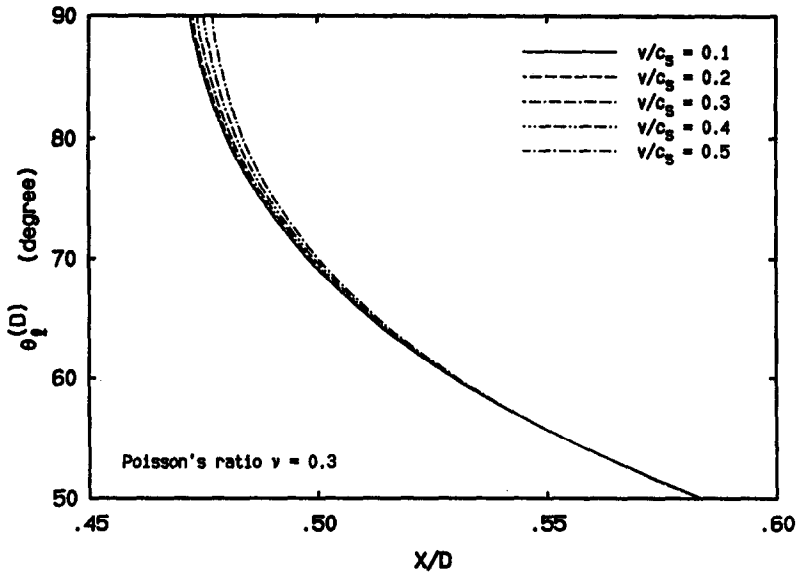

Fig. 5. Value of the parameter $\theta_1^{(D)}$, solved by eqn (26), versus the ratio X/D, for different crack-tip velocities.

that $\theta_1^{(D)}$ is a function of the ratio X/D only. Figure 5 presents the variation of the parameter $\theta_1^{(D)}$ versus the ratio X/D for different crack-tip propagating velocities. As we can see from this figure, the parameter $\theta_1^{(D)}$ is very sensitive to the ratio of X/D, but is not sensitive to the crack-tip velocity. The effect of transience on X/D is shown in Fig. 6. Figure 6 gives the variation relation between the ratio X/D and the non-dimensional parameter r_0/vt. It is shown that when the stress state around the crack tip deviates from K_1^d-dominance ($r_0/vt \to \infty$), the ratio X/D deviates from its steady-state value which implies that the caustic becomes more elongated in the X_1-direction due to the existence of transient effects for this particular problem. Since the parameter $\theta_1^{(D)}$ is very sensitive to the X/D, the accurate measurement of X and D becomes a crucial aspect of the new interpretation method.

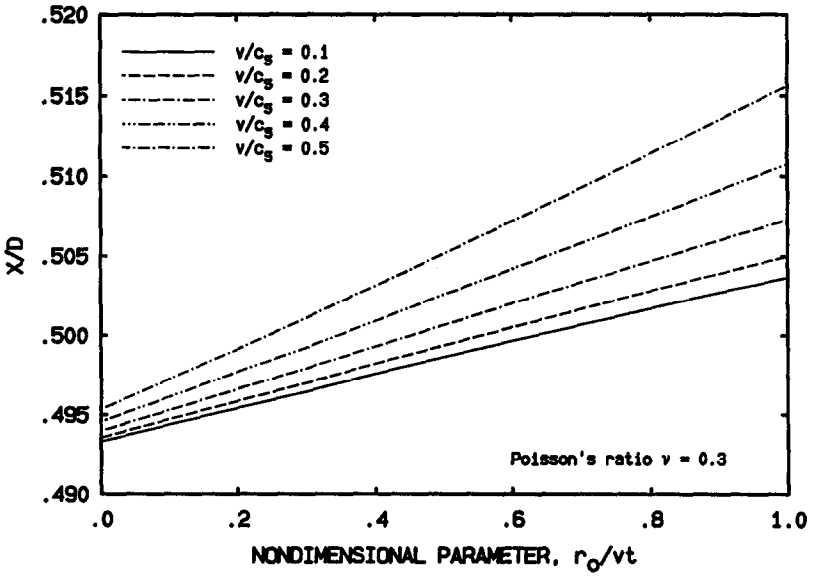

Fig. 6. Ratio X/D versus the non-dimensional parameter r_0/vt, for different crack-tip velocities.

Quantitative estimates of the error incurred by the classical interpretation of caustics during crack growth are presented in Fig. 7. Here the ratio $K^{d}_{I(caustic)}/K^{d}_{I(theo.)}$ is presented as a function of the parameter r_0/vt for different crack-tip velocities. As anticipated earlier, as $r_0/vt \to 0$ the classical analysis becomes accurate (either zero initial curve or a long time after initiation). However, as $r_0/vt \to \infty$, we observe large deviations of $K^{d}_{I(caustic)}$ relative to $K^{d}_{I(theo.)}$, which is known already (see lines with square symbols). The figure also presents the same ratio obtained if the numerically constructed caustics are analysed on the basis of our improved method [eqns (27) and (28)]. As is obvious from the lines marked by the circles, errors of less than 5%, which are acceptable in the experimental investigation of dynamic fracture mechanics, are obtained. In both cases it is shown that the effect of velocity is small especially when the improved analysis is used. The 5% relative error observed in this figure is caused by the assumption of circularity about the initial curve. Once again, the validity of this assumption is justified.

An alternative representation of the above results is given in Figs 8–10. Here $K^{d}_{I(caustic)}/K^{d}_{I(theo.)}$ is plotted versus time from crack initiation. The results of both improved and classical analyses of caustics are included. Figure 8 shows the variation of this ratio for a variety of crack-tip velocities for material parameters corresponding to 4340 steel, $z_0 = 2.0$ m, and specimen thickness $h = 0.01$ m. It indicates that the classical analysis of caustics becomes accurate only after a certain time from crack initiation. Figure 9 shows the same ratio as a function of time for different values of σ_∞/E, but the material parameters correspond to PMMA. This figure indicates that for a higher load level, the transient effect is much more significant than for the lower load level, especially at the time near the crack initiation. This reflects the fact that at a specific time t and fixed z_0, higher σ_∞/E implies larger initial curve radii [see eqn (44)]. It is seen from these two figures that as $t < 20\,\mu$s, big errors have been observed when the classical analysis is used. From the Broberg problem, we have $\dot{K}^{d}_{I}/K^{d}_{I} = 1/2t$. So for this particular problem, as $\dot{K}^{d}_{I}/K^{d}_{I} > 2.5 \times 10^4\,s^{-1}$, transient effects cannot be neglected, and this gives an estimate of $\dot{K}^{d}_{I}$ for which the improved method promises to provide accurate values of K^{d}_{I}.

Figure 10 shows the dependence of this ratio on z_0. Here, it is evident that as z_0 is decreased (the initial curve shrinks to the crack tip) the value of $K^{d}_{I(caustic)}$ obtained from the classical analysis of caustics slowly approaches $K^{d}_{I(theo.)}$. Nevertheless, large errors still persist near initiation. From the practical point of view, this is not a consolation since acceptable reductions of z_0 (and thus r_0) are limited by the size of the near tip three-dimensional zone

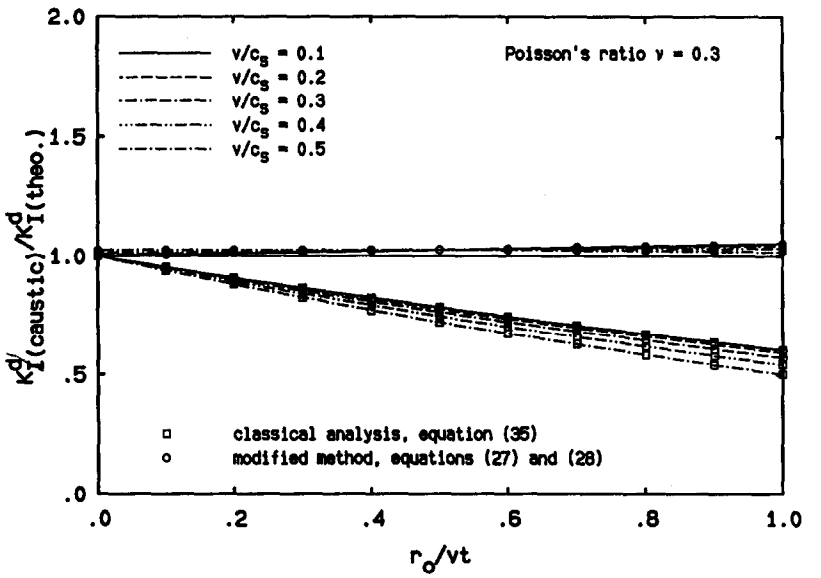

Fig. 7. Comparison of the dynamic stress intensity factor inferred from the modified method and the classical analysis for different values of r_0/vt, and for different crack-tip velocities.

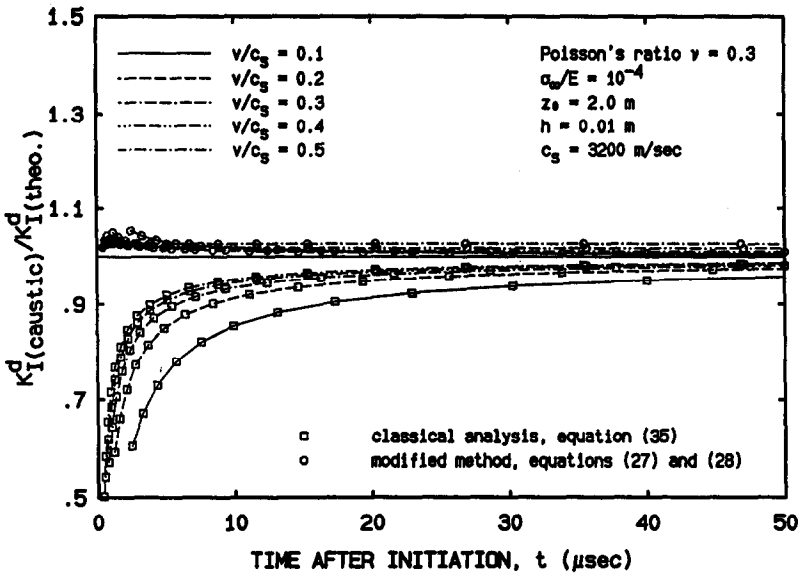

Fig. 8. Variations of the ratio $K^d_{I(caustic)}/K^d_{I(theo.)}$ with the time after crack initiation for different crack-tip velocities. The material parameters correspond to 4340 steel.

($\sim 0.5h$). Here the advantage of the modified interpretation becomes clear since accurate results can be obtained with relatively large values of z_0 corresponding to caustic measurements *outside* the near tip three-dimensional zone.

5. DISCUSSION AND CONCLUDING REMARKS

Motivated by recent experimental evidence (Krishnaswamy and Rosakis, 1991; Krishnaswamy *et al.*, 1992) that shows the inadequacy of the classical analysis of caustics in furnishing accurate values of K^d_I in the presence of transient effects, a modified analysis of the technique is presented here. This analysis is based on a fully transient higher order expansion recently developed by Freund and Rosakis (1992). The improved analysis of

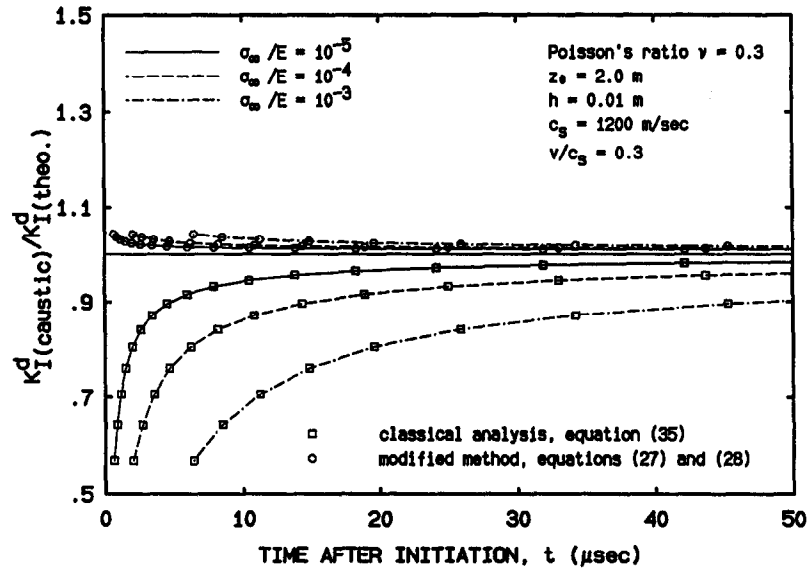

Fig. 9. Variations of the ratio $K^d_{I(caustic)}/K^d_{I(theo.)}$ with the time after crack initiation for different load levels, σ_∞/E.

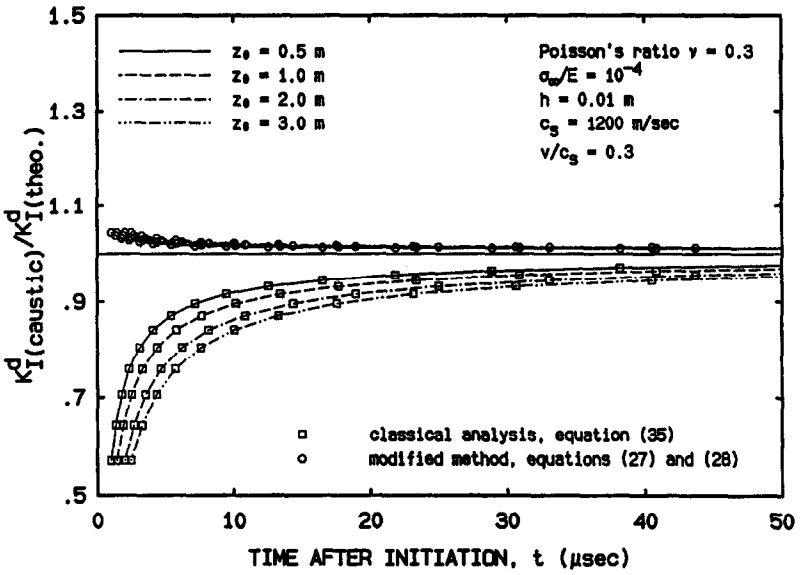

Fig. 10. Variations of the ratio $K^d_{I(caustic)}/K^d_{I(theo.)}$ with the time after crack initiation for varying experimental parameter z_0.

caustic patterns includes the influence of transients resulting because of the existence of non-uniform $K^d_I(t)$ and $v(t)$ histories [effects of $\dot{K}^d_I(t)$ and $\dot{v}(t)$]. The analysis can be used to obtain $K^d_I(t)$ as well as the values of higher order terms in terms of the geometrical characteristics of the caustic curves. The resulting expressions contain the classical results (static or dynamic K^d_I-dominant analyses) as special cases. The relative performance of the improved and the classical analyses is compared. This is done by considering the Broberg problem as an example model of transient crack growth. Based on the full Broberg solution, the caustic curves are first constructed numerically. These curves are then analysed to obtain $K^d_I(t)$, as would be done in an experiment, and to compare with the theoretically known $K^d_I(t)$ time history. When the caustics are analysed on the basis of eqn (35) (classical K^d_I-dominant analysis) very large errors are obtained at times close to crack initiation. As a matter of fact, for this problem, such errors are unbounded as $t \to 0$. On the other hand, when eqns (27) and (28) are used in the analysis of the caustic patterns, the measured $K^d_I(t)$ agrees very well with the theoretical value (to within 5%). This clearly indicates that the improved analysis of caustics, based on the higher order transient expansion, is capable of providing accurately the dynamic stress intensity factor history even if the crack growth event is very transient.

Another noteworthy fact is that the crack-tip propagating velocity is assumed to be known in the analysis. However in real applications, the crack-tip position is only approximately known, since the crack tip is covered by the dark shadow spot. This problem can be overcome either by simultaneously using some other measurement techniques which can provide the crack-tip position at each instant of time, or by the following iteration procedure. At the beginning of the iteration process, we can assume that the caustic diameter D passes through the crack tip. As a result, X represents the distance from the crack tip to the front of the caustic curve. After the crack-tip position is determined by this assumption, an approximate crack-tip velocity history can be deduced. By carrying out the measurement method we proposed in Section 3.2, all parameters will be determined. If we now go back to eqn (8) to calculate the "real" distance from the crack tip to the caustic front, then the velocity history will be corrected. This procedure will be repeated until the crack-tip velocity converges at each instant of time.

The shortcomings of the classical analysis of caustics discussed in this paper may have far-reaching consequences. In particular, caution should be exercised in the interpretation of experimental measurements obtained by caustics in the past, especially when highly transient crack problems were studied by the technique.

During the past two decades, the optical method of caustics has been widely used in experimental solid mechanics, especially in the study of dynamic fracture processes. Another method, which is also widely adopted, is photoelasticity. The history of photoelasticity is much longer than the method of caustics and therefore can be thought of as well developed. Nevertheless, due to the simplicity of the method of caustics either in the experimental set up, or in the data analysis, both techniques remain appealing as powerful candidates in the study of fracture processes. However serious discrepancies have been reported in the literature by a number of researchers using the classical interpretation of caustics or photoelasticity. Nigam and Shukla (1988) have compared the methods of photoelasticity and transmission caustics by performing experiments on identical specimens under identical loading. Their results show that while both methods work well for static problems, the method of photoelasticity gives values for the dynamic stress intensity factor which vary by about 30–50% from those obtained through the method of caustics. In this paper, we have shown by using the Broberg problem, that for transient crack propagation with constant velocity, the value of the dynamic stress intensity factor obtained through the classical analysis of caustics can indeed produce differences of that magnitude or even higher. This provides a qualitative explanation of the different results in $K_I^d(t)$ obtained from these two techniques in Nigam and Shukla's paper. It should be pointed out that in the interpretation of their photoelastic fringes, Nigam and Shukla used a two-dimensional "higher-order" expansion suggested by Dally *et al.* (1985). This expansion is based on the steady-state asymptotic representation of the stresses around the crack tip. As was shown in this paper, only at the region very close to the crack tip, the transient effects will not be felt strongly. Outside this region the dynamic transient effects will affect the stress distribution. This issue was also discussed by Krishnaswamy *et al.* (1990) by using the CGS method. It has also been shown by Rosakis *et al.* (1991), that the asymptotic expansion of stresses under the fully transient condition is different from that obtained under the steady-state condition. The steady-state, higher-order expansion can be approximately used only when the time derivatives of all the coefficients are negligibly small and the crack-tip velocity is essentially constant. If these conditions are violated, the results of the steady-state approximation are questionable. Nonetheless, the use of a higher order steady state expansion is bound to be an improvement over the assumption of strict K_I^d-dominance. As a result, the values of $K_I^d(t)$ obtained by photoelasticity in Nigam and Shukla's paper are expected to be close to the real value of K_I^d rather than the one obtained by the classical analysis of caustics.

A long-standing issue of fundamental importance in dynamic fracture research is the connection between the dynamic fracture toughness, K_{IC}^d, and the crack-tip velocity. The debate, for the most part, has centered around the question of whether a unique, material dependent relationship exists between K_{IC}^d and v. Kobayashi and Dally (1980), Rosakis *et al.* (1984) and Zehnder and Rosakis (1990), among others, provide data sets that seem to indicate that a relation between K_{IC}^d and v exists and may reasonably be viewed as a material property. For most materials tested, K_{IC}^d was found to be a weakly increasing function of crack-tip velocity, for low velocities, followed by a strongly increasing branch as the crack speed increases. The location of the steep branch depends on the material under consideration. The conclusion of the existence of a unique curve is usually made in the presence of experimental scatter in both K_{IC}^d and $v(t)$. In particular, it should be emphasized here that the data sets provided by Rosakis *et al.* (1984) and Zehnder and Rosakis (1990) for AISI carbon steel, *if collectively viewed,* are characterized by a scatter in K_{IC}^d of the order of 30% for crack-tip velocities in the range of 400–900 m s^{-1}. Nonetheless it should also be remembered that the dynamic stress intensity factor was inferred by using the classical analysis of caustics which assumes K_I^d-dominance and neglects the history dependent, transient nature of the field. In addition, it should be recalled that two different specimen and loading geometries were used. Further, even within one specimen geometry, the resulting crack growth histories were intentionally varied (by controlling the starter notch radius), in order to span a representative range of crack-tip velocities. This is a common practice of most experimental investigations in this field. The above observations clearly indicate that each of these experiments was characterized by very distinct transient

crack growth histories. Finally, and as was observed by Zehnder and Rosakis (1990), if data from a *single* specimen were used to explore the variation of K^d_{IC} and v, very smooth curves resulted. However if such variations were collectively viewed, then the resulting data scatter was of the order of 30% in K^d_{IC}.

Given the above observations, it is therefore conceivable that the observed maximum scatter between tests may be due to phenomena of the type observed in this paper, i.e. errors associated with the classical analysis of caustics when strict K^d_I-dominance is violated.

Another series of experiments leading to results that have yet to be explained are those reported by Dahlberg *et al.* (1980) and Kalthoff (1983), which seem to indicate that the dynamic fracture toughness could be specimen dependent. The claim of specimen dependence is made in the presence of 20% differences between curves obtained for each specimen configuration. In this case, as well, the observations related to the work of Rosakis *et al.* (1984) and of Zehnder and Rosakis (1990) are relevant. Here again the crack growth histories varies from configuration to configuration and from specimen to specimen. As a result, it may be possible to attribute the apparent specimen dependence of K^d_{IC} vs v to the specimen dependent transient nature of the region where the caustic measurement was made.

On the basis of some crack propagation experiments in which the optical method of caustics was used, Takahashi and Arakawa (1987) proposed that the instantaneous value of dynamic fracture toughness of their material depended on the instantaneous crack-tip acceleration. As shown in Freund and Rosakis (1992) and Rosakis *et al.* (1991), however, the near tip stress field expansion involves crack-tip acceleration in its third or higher order terms. As a result, caustic patterns obtained from regions where higher order terms are important will exhibit acceleration effects. However, if caustics from such a region are *interpreted* on the assumption of K^d_I-dominance then it would appear that the instantaneous value of stress intensity factor, and thus of fracture toughness of the material, depends on the instantaneous acceleration of the crack tip.

The above comments are also relevant to the works of Kobayashi and Mall (1978) and Ravi-Chandar and Knauss (1984) who suggested that although an average increasing trend in K^d_{IC} with crack-tip velocity seems to exist, no clear, unique relation between K^d_{IC} and v could be found. Here again the question of transients in the interpretation of caustics becomes important. As discussed by Freund and Rosakis (1992), this becomes more transparent in the second reference, since there, the analytical time history of K^d_I is available to be compared with the one inferred based on caustics. Indeed it is shown that the classical analysis of caustics is adequate in predicting $K^d_I(t)$ during loading, up to the point of crack initiation. After initiation of dynamic crack growth differences of over 50% to the theoretical value are seen.

We would like to conclude this discussion by pointing out that the above observations on past experimentation (including our own work) are by no means meant to discredit the use of caustics as an experimental tool in dynamic fracture studies. On the contrary we attempt to provide means to improve the accuracy of interpretation of this method which we believe to be a formidable tool for the study of transient crack problems. Indeed, given the extraordinary experimental simplicity of the technique and the large numbers of raw re-analysable data already available, this seemed to be a worthwhile task. In addition, we believe that the time for taking final positions in the debate regarding the existence of a unique K^d_{IC} vs v curve has not arrived yet. Our current observations merely suggest that the existing arguments (including our own in the past) based on experimental interpretations (for both photoelasticity and caustics) which neglect the transient nature of crack growth cannot be conclusive. We believe that further experimental study or even re-interpretation of raw experimental measurements using the recently available transient results is required to assess the possibilities and to resolve this issue once and for all.

Acknowledgements—The authors would like to acknowledge the support of the Office of Naval Research through ONR Grand N00014-90-J-1340.

REFERENCES

Beinert, J. and Kalthoff, J. F. (1981). Experimental determination of dynamic stress-intensity factors by the method of shadow patterns. In *Mechanics of Fracture* (Edited by G. C. Shih), Vol. VII, pp. 281–330. Martinus Nijhoff, The Hague.

Broberg, K. B. (1960). The propagation of a brittle crack. *Archiv. für Fysik* **18,** 159–192.

Dahlberg, L., Nilsson, F. and Brickstad, B. (1980). Influence of specimen geometry on crack propagation and arrest toughness. In *Crack Arrest Methodology and Applications* (Edited by G. T. Hahn and M. F. Kanninen), ASTM STP 711, pp. 89–108.

Dally, J. W., Fourney, W. L. and Irwin, G. R. (1985). On the uniqueness of K_{ID}–$\dot{a}$ relation. *Int. J. Fracture* **27,** 159–168.

Freund, L. B. (1990). *Dynamic Fracture Mechanics*. Cambridge University Press, Cambridge.

Freund, L. B. and Rosakis, A. J. (1990). The influence of transient effects on the asymptotic crack tip field during dynamic crack growth. Eleventh National Congress of Applied Mechanics, Tucson, Arizona, May.

Freund, L. B. and Rosakis, A. J. (1992). The structure of the near tip field during transient elastodynamic crack growth. *J. Mech. Phys. Solids* **40**(3), 699–719.

Goldsmith, W. and Katsamanis, F. (1979). Fracture of notched polymeric beams due to central impact. *Experimental Mech.* **18,** 235–244.

Kalthoff, J. F. (1983). On some current problems in experimental fracture mechanics. In *Workshop on Dynamic Fracture* (Edited by W. G. Knauss *et al.*), pp. 11–35. California Institute of Technology.

Kalthoff, J. F., Beinert, J. and Winkler, S. (1978). Influence of dynamic effects on crack arrest. Institut für Festkörpermechanik, Tech. Report, August.

Kalthoff, J. F., Winkler, S. and Beinert, J. (1976). Dynamic stress—intensity factors for arresting cracks in DCB specimens. *Int. J. Fracture* **12,** 317–319.

Katsamanis, F., Raftopoulos, D. and Theocaris, P. S. (1977). Static and dynamic stress intensity factors by the method of transmitted caustics. *J. Engng Mater. Tech.* **99,** 105–109.

Kobayashi, T. and Dally, J. W. (1980). Dynamic photo-elastic determination of the $\dot{a}$–K relation for the 4340 steel. In *Crack Arrest Methodology and Applications* (Edited by G. T. Hahn and M. F. Kanninen), ASTM STP 711, pp. 189–210.

Kobayashi, A. S. and Mall, S. (1978). Dynamic fracture toughness of homalite 100. *Exp. Mech.* **18,** 11–18.

Krishnaswamy, S. and Rosakis. A. J. (1991). On the extent of dominance of asymptotic elastodynamic crack-tip fields: Part I—An experimental study using bifocal caustics. *J. Appl. Mech.* **58**(1), 87–94.

Krishnaswamy, S., Tippur, H. V. and Rosakis, A. J. (1992). Measurement of transient crack tip deformation fields using the method of coherent gradient sensing. Caltech Report SM 90-1. *J. Mech. Phys. Solids* **40**(2), 339–372.

Manogg, P. (1964). Anwendungen der Schattenoptik zur Untersuchung des Zerreissvorgags von Platten. Dissertationsschrift an der Universität Freiburg, Germany.

Nigam, H. and Shukla, A. (1988). Comparison of the techniques of transmitted caustics and photoelasticity as applied to fracture. *Experimental Mech.* **28**(2), 123–133.

Ravi-Chandar, K. and Knauss, W. G. (1984). An experimental investigation into the mechanics of dynamic fracture: I. Crack initiation and arrest. *Int. J. Fracture* **25,** 247–262.

Rosakis, A. J. (1980). Analysis of the optical method of caustics for dynamic crack propagation. *Engng Fract. Mech.* **13,** 331–347.

Rosakis, A. J. (1992). Two optical techniques sensitive to gradients of optical path difference: The method of caustics and the coherent gradient sensor (C.G.S.). In *Experimental Techniques in Fracture* (Edited by J. Eptein), Vol. III.

Rosakis, A. J., Duffy, J. and Freund, L. B. (1984). The determination of dynamic fracture toughness of AISI 4340 steel by the shadow spot method. *J. Mech. Phys. Solids* **32,** 443–460.

Rosakis, A. J., Krishnaswamy, S. and Tippur, H. V. (1990). On the application of the optical method of caustics of the investigation of transient elastodynamic crack problems: Limitations of the classical interpretation. *Optics Lasers Engng* **13,** 183–210.

Rosakis, A. J., Liu, C. and Freund, L. B. (1991). A note on the asymptotic stress field of a non-uniformly propagating dynamic crack. *Int. J. Fracture* **50,** R39–R45.

Rosakis, A. J. and Ravi-Chandar, K. (1986). On crack-tip stress state: An experimental evaluation of three-dimensional effects. *Int. J. Solids Structures* **22**(2), 121–134.

Rosakis, A. J. and Zehnder, A. T. (1985). On the method of caustics: An exact analysis based on geometrical optics. *J. Elasticity* **15**(4), 347–368.

Schardin, H. (1959). Velocity effects in fracture. In *Fracture* (Edited by B. L. Averback *et al.*). John Wiley and Sons, New York.

Takahashi, K. and Arakawa, K. (1987). Dependence of crack acceleration on the dynamic stress-intensity factor in polymers. *Experimental Mech.* **27**(2), 195–199.

Theocaris, P. S. (1970). Local yielding around a crack tip in plexiglass. *J. Appl. Mech.* **37,** 409–415.

Theocaris, P. S. (1971). Reflected shadow method for the study of constrained zones in cracked plates. *Appl. Optics* **10,** 2240–2247.

Theocaris, P. S. (1981). Elastic stress intensity factors evaluated by caustics. In *Mechanics of Fracture* (Edited by G. C. Sih), Vol. VII, pp. 253–280. Martinus Nijhoff, The Hague.

Theocaris, P. S. (1978). Dynamic propagation and arrest measurements by the method of caustics on overlapping skew-parallel cracks. *Int. J. Solids Structures* **14,** 639–653.

Theocaris, P. S. and Gdoutos, E. E. (1974). The modified Dugdale–Barenblatt model adapted to various fracture configurations in metals. *Int. J. Fracture* **10,** 549–564.

Yang, W. and Freund, L. B. (1985). Transverse shear effects for through cracks in an elastic plates. *Int. J. Solids Structures* **21**(9), 977–994.

Zehnder, A. T. and Rosakis, A. J. (1990). Dynamic fracture initiation and propagation in 4340 steel under impact loading. *Int. J. Fracture* **43**(4), 271–285.